AIAA-2001-1388

LOW VELOCITY EARTH-PENETRATION TEST AND ANALYSIS

Edwin L. Fasanella*
US Army Research Laboratory, Vehicle Technology Directorate
Hampton, VA 23681

Yvonne Jones†
NASA Langley Research Center
Hampton, VA 23681

Norman F. Knight, Jr.‡ and Sotiris Kellas§
Veridian Systems
Yorktown, VA

Abstract

Modeling and simulation of structural impacts into soil continue to challenge analysts to develop accurate material models and detailed analytical simulations to predict the soil penetration event. This paper discusses finite element modeling of a series of penetrometer drop tests into soft clay. Parametric studies are performed with penetrometers of varying diameters, masses, and impact speeds to a maximum of 45 m/s. Parameters influencing the simulation such as the contact penalty factor and the material model representing the soil are also studied. An empirical relationship between key parameters is developed and is shown to correlate experimental and analytical results quite well. The results provide preliminary design guidelines for Earth impact that may be useful for future space exploration sample return missions.

Introduction

Future space science missions will involve the acquisition, storage, and return of sample material collected during space flight or planetary exploration [1]. These sample return missions will require the design of reliable Earth entry vehicles. Currently, different configurations are being studied for such vehicles with the design requirement to survive a guided impact with selected areas of the Earth's surface without the aid of a parachute. Developing an understanding of this impact scenario will provide added robustness to the vehicle design and increased reliability of the system.

An advanced technology test program has been developed to meet this challenge. The program will provide important test results for the overall vehicle design and also for validating analytical simulation tools. Low-velocity penetrometer drop tests were performed in November 1998 at the Utah Test and Training Range (UTTR) into soft clay from a bucket truck and a hot-air balloon. Also, a series of drop tests were performed from a helicopter onto soil at impact velocities up to 45 m/s at UTTR in September 2000. Hemispherical penetrometers of varying diameter were dropped to provide selected data for a range of design parameters to support sample return missions. Some limited penetration and soil sampling data from the late 1960's for low-velocity Earth impact into soft clay are also available in references [2,3]. The impact data and soil analysis in reference [2] was for the UTTR site, but focused on long slender impactors with deep penetrations.

* Structural Dynamics Branch, NASA LaRC. Member AHS
† Engineering Co-op, University of Tennessee
‡ Staff Scientist. Associate Fellow AIAA.
§ Principal Engineer.

The focus of this paper is to describe the development of the soil impact simulation and the correlation between the numerical results and the penetrometer test data. The modeling approach for the penetrometer test, the material model for the soil, and the influence of key analysis parameters on the simulations are described. An empirical relationship is developed to predict the peak acceleration based on penetrometer size, mass, and impact velocity. MSC.Dytran [4] is used to simulate these drop tests and to predict additional results when test data are not available.

Drop Test Data from UTTR

Data from penetrometer drop tests conducted at UTTR from a bucket truck and a hot-air balloon in 1998 and from a helicopter in 2000 are summarized in Table I. Each penetrometer is hemispherical-shaped with an internal high-speed (>100k samples/s) digital data acquisition system to record the acceleration time history. Penetrometers with diameters ranging from 0.203 to 0.66 meters were used with velocities ranging from 5.74 to 45 m/s. The total penetrometer mass varied from 2.98 to 24.5 kg.

A post-test photo of the 0.408-m penetrometer with crater after a 45 m/s impact at UTTR in September 2000 is shown in Figure 1.

Fig. 1. Post-test picture of 0.408-m penetrometer after 45m/s impact (September 2000 at UTTR).

Finite Element Modeling

The analysis was performed using the software program MSC.Dytran. MSC.Dytran is an explicit, nonlinear transient dynamic finite element computer code with its origins related to the public-domain DYNA3D code developed at Lawrence Livermore National Laboratory. The input format for MSC.Dytran was made to be as compatible as practical with MSC.Nastran. MSC.Dytran offers a library of structural elements (beams, shells, and solids) for modeling complex structures. MSC.Dytran also offers a variety of models for elastic, elasto-plastic, and layered orthotropic materials, and for crushable foams and soils; thereby allowing most engineering material systems to be analyzed. Several modeling options are available for contact, impact, and penetration including breakable joints and element erosion. Automatic time step control is provided once the user defines an acceptable initial time step. Archive files for post-processing data into deformed shapes and time history files to generate xy-plots of selected grid points, material variables, or contact variables must be requested by the user. A restart capability is also provided.

Table I – Test Matrix of Penetrometer drops at UTTR

Diam. (m)	Mass (kg)	Vel. (m/s)	Peak Accel (g's)	Test Helicopter/2000 Others/1998
0.203	2.98	5.74	85	1 drop hammer
0.408	12.05	34.97	1195	2 helicopter
0.408	12.05	43.15	1482	3 helicopter
0.408	12.05	44.9	1656	4 helicopter
0.408	24.5	31.94	614	5 helicopter
0.408	24.5	39.42	812	6 helicopter
0.408	24.5	45.35	1016	7 helicopter
0.514	11.02	16.7	500	8 bucket truck
0.514	18.54	19.1	300	9 bucket truck
0.514	18.91	16.7	210	10 bucket truck
0.514	18.91	21.8	325	11 balloon
0.514	18.91	25.9	510	12 balloon
0.66	24.0	35	1080	13 helicopter
0.66	24.0	40	1295	14 helicopter

Finite Element Discretization

The finite element model of the penetrometer and soil is shown in Figure 2. The penetrometer consists of an aluminum shell with a series of reinforcing internal ribs and a mount for the digital instrumentation package. In these simulations, the penetrometer is represented as a rigid body with a given mass and initial impact velocity. In order to represent the geometry accurately, the rigid-body hemispherical penetrometer was discretized into a fine mesh of 1, 200 shell elements.

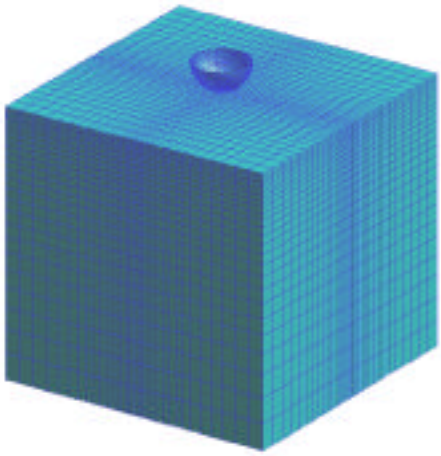

(a) Full model.

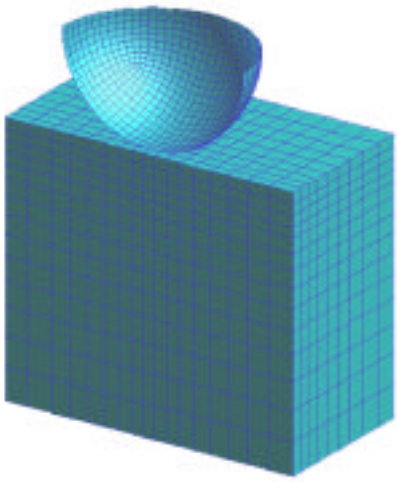

(b) Close-up section of model.

Fig. 2. Penetrometer/soil finite element model.

The soil is modeled as a hexagonal-shaped region with dimensions of approximately five times the penetrometer radius on each side. The spatial discretization provides a graded mesh with smaller elements near the top-center surface where the impact will occur. The graded mesh is generated using the two-way bias mesh seed of MSC.Patran with an element side length in the top center region being five times smaller than those at the bounding surfaces. There are 33 elements of varying size along the length of each side of the soil model. In the full model, the soil is discretized into 27,225 8-node solid single-integration-point elements. The nodes on the outer vertical surfaces of the soil are allowed to be free, while the nodes on the bottom surface are fully restrained. The total number of nodes in the model including both the soil and penetrometer is 31,380.

In the vertical direction, the soil model is divided into two layers. The top layer is approximately 1/5 of a penetrometer radius deep, and the bottom layer consists of the rest of the soil. The properties of the top layer of soil could differ significantly from the deeper soil. This approach was used to represent the soil at UTTR, which is typically characterized by a dry upper layer, while the lower layer may be saturated with water.

Soil Constitutive Model

The soil was modeled as an elastic-plastic material with strain hardening (DYMAT24). The nominal values used to characterize the soil were: an elastic secant modulus E equal to 4000 kPa, Poisson's ratio ν equal to 0.3, a yield stress (or bearing pressure) σ_y equal to 68.9 kPa, and mass density 2201.6 kg/m^3 based on a 65% moisture content. A hardening modulus EH of 800 kPa (0.2E) was used in the final model. Soil near the surface is estimated to have a moisture content of approximately 22% during dry conditions. This soil model is an approximation to the actual soil properties and was used due to limited data to characterize the soil. Most of the UTTR soil properties were obtained using the charts in reference [2], and from information using soft clay surrogates in the laboratory. The simple elastic-plastic material model of the soil was quite successful in predicting the UTTR test acceleration pulses and was recommended in several references [5,6]. Improved correlation was obtained with the portion of the experimental acceleration pulse after the peak by including strain hardening. More complex material models for the soil such as the cap model [7] were also considered. However, the coefficients and parameters needed for the cap model could not be determined given the available data.

Contact Modeling

Contact between the rigid-body penetrometer and the soil is modeled using the penalty method with the bounding top surface of the soil serving as the master contact surface. The nodes on the rigid penetrometer were defined as the slave nodes. Note that contact between a rigid body and a deformable body can cause numerical problems. However, the use of a rigid body may speed up the analysis by an order of magnitude. Generally, a master contact surface can be coarsely discretized. However, since the master surface (soil surface) deforms significantly, the discretization of the master surface is quite important for this problem. Thus, the mesh in the contact zone must be reasonably fine. Some of the other contact parameters in MSC.Dytran include the type of contact (VERSION), the weighting factor (WEIGHT), the selection of the monitoring side

(SIDE), and the contact penalty factor (FACT). The results presented in this paper used VERSION=V4, WEIGHT=SLAVE, and SIDE=BOTH.

The parameter FACT is quite important as it represents a scale factor for the contact force. When a slave node penetrates the master surface too deeply, the contact can be made stiffer by increasing FACT. However, for dissimilar materials with significantly differing stiffnesses, even the default value of FACT (0.1) may lead to a large contact force that may artificially over accelerate the less dense material. Such a result could cause a separation between the slave node and master surface until the slave nodes "catch up" to the master surface again. Monitoring the position of adjacent nodes on the master surface and corresponding slave nodes aids in identifying this numerical artifact of the contact simulation. If the separation distance becomes too large, the value of FACT may be reduced to decrease the likelihood of excess separation between the contact surfaces.

Numerical Results and Discussion

Selected penetrometer drop tests into clay were simulated pre-test, and later the analytical results were correlated with the test data from UTTR. The matrix of drop tests is shown in Table I. The simulations were performed using MSC.Dytran Version 2000 on a Sun Enterprise 450 Unix workstation. A typical simulation was executed for 25 ms of actual time using a maximum time step of 10 microseconds and required about one CPU hour.

Soil Discretization and Contact Penalty Factor

The discretization of the soil beneath the penetrometer (i.e., in the contact zone) and the contact penalty factor are both critical in achieving good analytical results. If the soil is discretized too coarsely in the contact zone and/or the contact penalty factor is too large, the resulting penetrometer acceleration may look like a series of spikes. When the contact force is too large, the soil is accelerated ahead of the penetrometer. Each time the penetrometer catches up with the soil, another acceleration spike occurs. The contact zone mesh discretization was varied to determine its effect using the default penalty factor (FACT). The results for a 0.2-m diameter, 2.98-kg penetrometer with impact velocity of 5.74 m/s are shown in Figure 3. For the results in Figures 3a and b, the master surface mesh beneath the sphere was coarse with only 25 element faces in the contact zone directly beneath the penetrometer. The acceleration response of the penetrometer shown in Figure 3a is a series of spikes, and the velocity response in Figure 3b resembles an increasing step function. This response illustrates the repeated contact and separation that occurs due to excessive contact force.

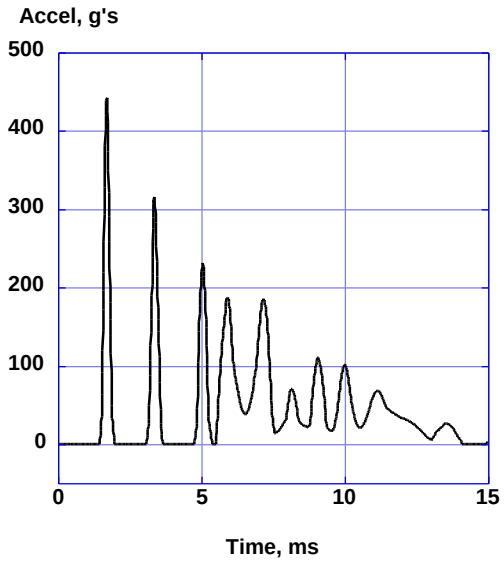

(a) Acceleration.

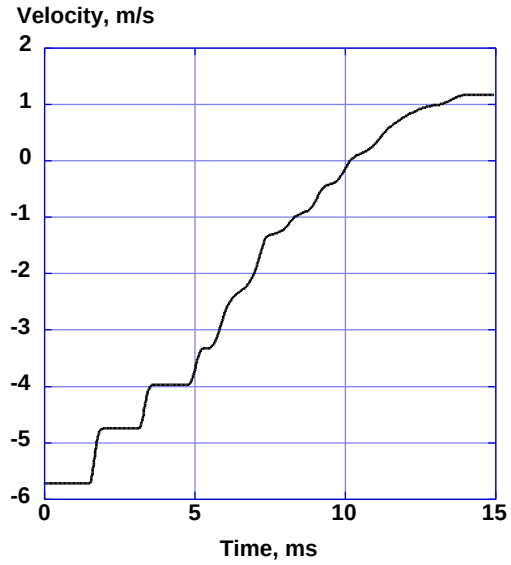

(b) Velocity.

Fig. 3. Acceleration and velocity time histories for the coarse contact zone model using FACT = 0.1.

A refined model of the soil with approximately 120 elements in the contact zone was analyzed to determine the effect of contact zone discretization. Results shown in Figure 4 for the refined contact zone model differ significantly from those in Figure

3. The “stair step” behavior in the velocity time history is replaced with a smooth curve. However, the acceleration response exhibits high peaks and high frequency oscillations superimposed on the basic acceleration pulse.

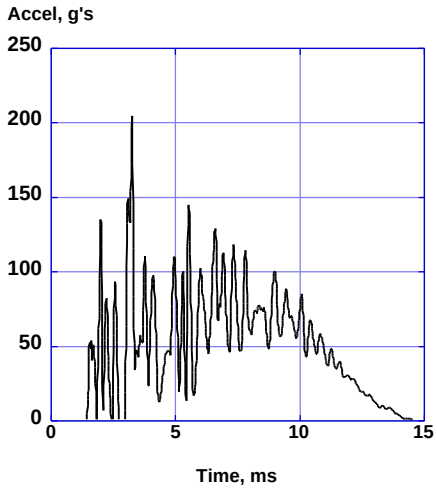

(a) Acceleration.

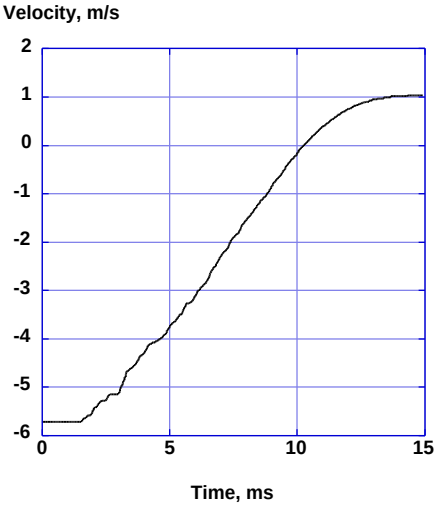

(b) Velocity.

Fig. 4. Acceleration and velocity time histories for the refined contact zone model using FACT = 0.1

The effect of the contact penalty factor (FACT) on the acceleration and velocity time histories for the coarse and refined contact zone models is shown in Figures 5 and 6, respectively. The response is now more characteristic of penetration transient response. Changing the value of FACT to 0.001 is needed due to the large difference in stiffness between the penetrometer (rigid) and the soil (very weak). The acceleration time histories shown in Figures 5a and 6a are similar, hence subsequent simulations use FACT = 0.001 (and with contact zone refinement). All velocity time histories in Figures 3 - 5 exhibited a direction change at approximately 10 ms and a final rebound velocity of 1 m/s.

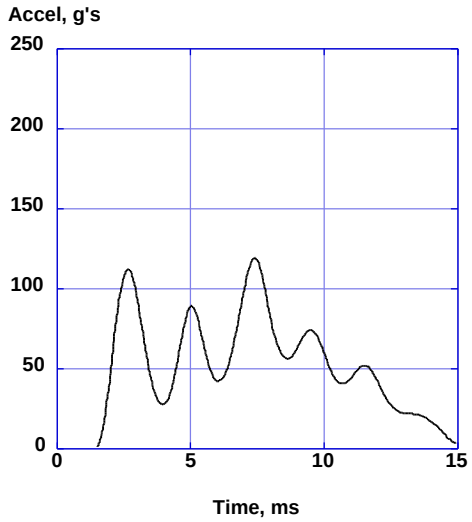

(a) Acceleration.

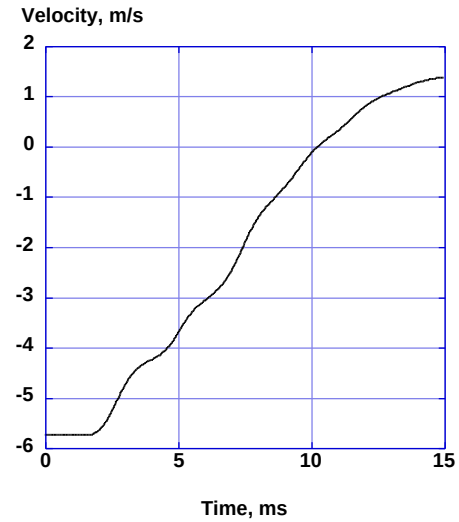

(b) Velocity.

Fig. 5. Acceleration and velocity time histories for the coarse contact zone model using FACT = 0.001.

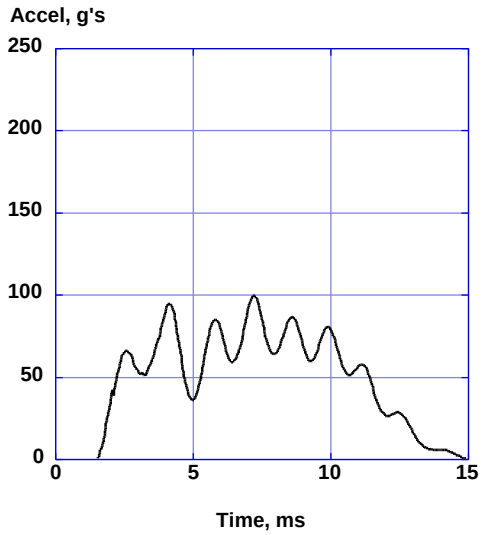

(a) Acceleration.

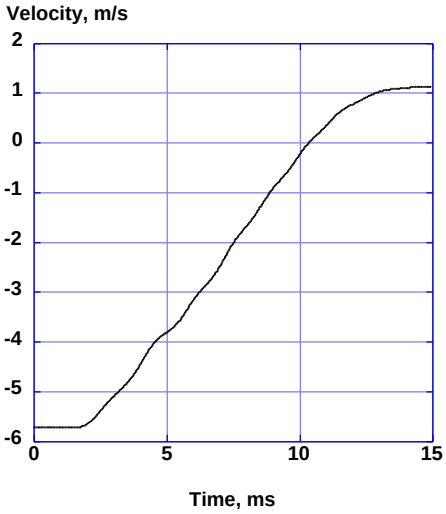

(b) Velocity.

Fig. 6. Acceleration and velocity time histories for refined contact zone model using FACT = 0.001.

Size and Velocity Effects

Next, a larger diameter penetrometer with a higher impact velocity is studied. The impact and penetration event for the 0.408-m diameter penetrometer with a mass of 12 kg and an initial velocity of 35 m/s can also be used to illustrate the effects of altering the contact penalty factor FACT in MSC.Dytran. The simulation was executed for 15 ms of real time using a maximum time step of 10 microseconds. The soil model for this case and the remainder of the simulations has 27,225 8-node solid brick elements with single-point integration. The contact zone for this case has approximately 80 element faces beneath the sphere. The rigid penetrometer is again discretized with 1,200 4-node shell elements to represent the surface contour accurately. For the acceleration time histories shown in Figure 7, the default value of 0.1 was first used for the contact penalty factor. However, adjacent nodes on the penetrometer and soil were found to move apart rather than stay in contact. When the contact factor was reduced to 0.001, the node at the bottom of the sphere and an adjacent node on the soil were found to move together, and the resulting rigid-body penetrometer acceleration response is smoothed without the requirement for digital filtering.

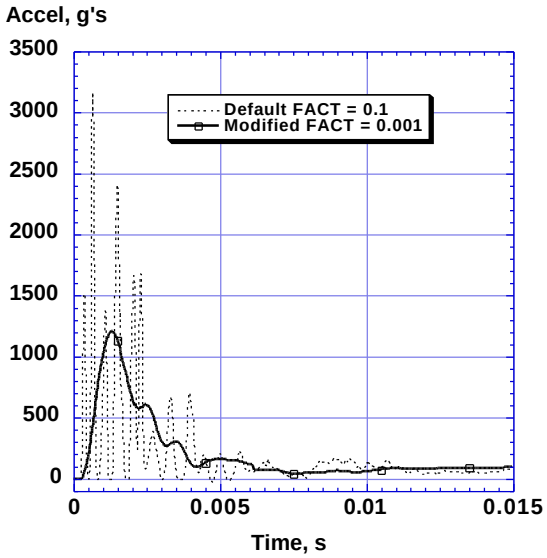

Fig. 7. Effect of penalty factor (FACT) on acceleration time history of penetrometer.

Effect of Soil Material Model

Using the elastic-perfectly plastic model, soil material parameters were varied to determine the effects on the acceleration pulse. If either the elastic modulus or the yield stress of the soil were varied by 20%, the influence on the resulting acceleration pulse was minimal. However, the effect of lowering the soil density by 20% from the nominal reduced the peak acceleration by approximately 20% as shown in Figure 8. Thus, the density of the soil is an important factor in the simulation. Drier soil, such as was found on the top layer at UTTR, is less dense than the bottom layers of soil, which may be saturated with water.

The acceleration response in Figure 8 for a 0.408-m diameter penetrometer weighing 12 kg with an impact velocity of 35 m/s was a pre-test prediction. The acceleration peak (1200 g's) for nominal density

matched the test data very well, but the drop off of the acceleration after the peak was too sharp when compared with the test data. The pre-test soil model was elastic-perfectly plastic. As is evident in Figure 9, when a hardening modulus (EH) of 20% of E was added to the material model, the peak value was not changed, but the acceleration drop off matched the test data more closely. The experimental acceleration response shown in Figure 9 was integrated to obtain velocity and penetration depth. The predicted penetration depth illustrated in Figure 9 (b) compared will with the integrated experimental value. Before the hardening modulus was introduced to simulate soil compaction, the analytical penetration was too deep.

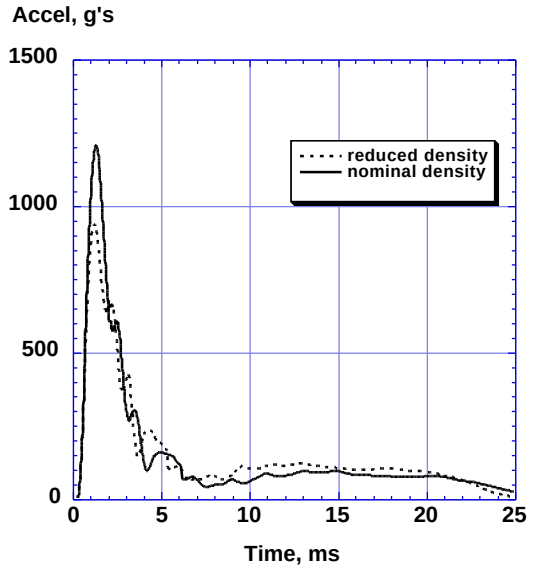

Fig. 8. Effect of clay density on peak acceleration for .408-m penetrometer with 12-kg total mass and impact velocity of 35 m/s.

Comparisons of Test with Analysis

Additional comparisons between test and analysis (with and without strain hardening) are shown in Figures 10 - 12. The predicted acceleration peaks match the experimental data quite well, and generally are within 10 to 15 percent of the experimental values. The pulse shape and duration are also simulated quite well, especially when strain hardening is included. These results indicate that the peak acceleration for a penetrometer of fixed size and mass increases as the initial impact velocity increases. For a fixed initial impact velocity, the peak acceleration decreases as the penetrometer size and mass increase.

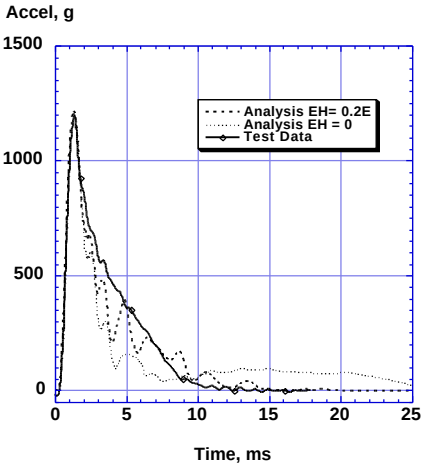

(a) Acceleration comparisons.

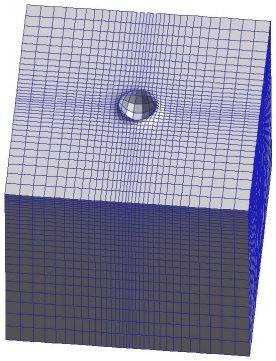

(b) Crater shown in soil model.

Fig. 9. Comparison of test with predicted acceleration pulse for the 0.408-m penetrometer with 12-kg total mass and impact velocity of 35 m/s.

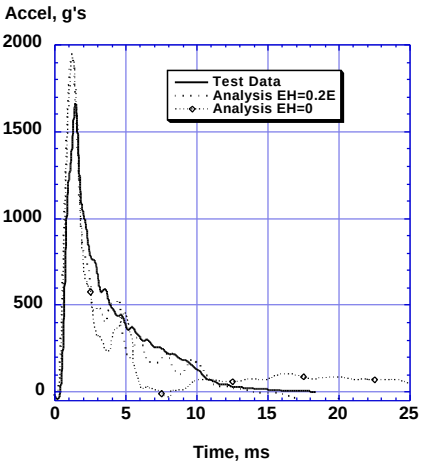

Fig. 10. Comparison of test with analysis of the 0.408-m penetrometer with 12-kg total mass and impact velocity of 45 m/s.

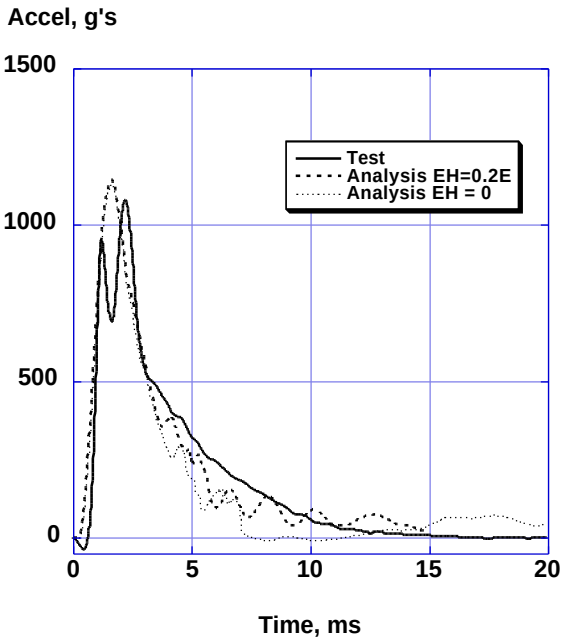

Fig. 11. Comparison of test with predicted acceleration pulse for 0.66-m penetrometer with 24-kg total mass and impact velocity of 35 m/s.

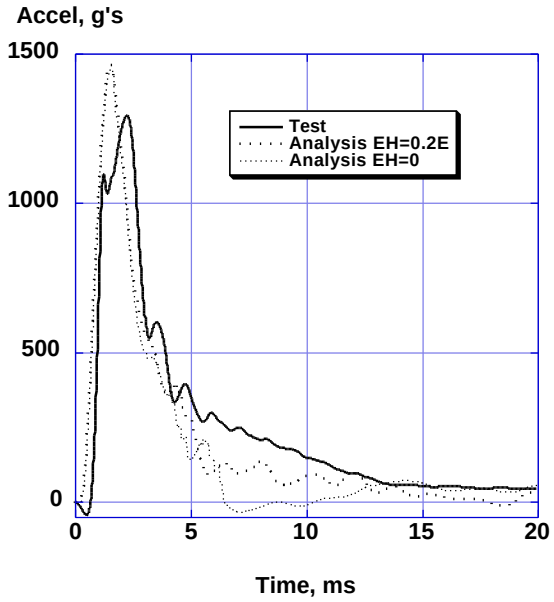

Fig. 12. Comparison of test with predicted acceleration pulse for 0.66-m penetrometer with 24-kg total mass and impact velocity of 40 m/s.

Empirical Relationship for Peak Acceleration

Based on test results and analysis, it was deduced that the peak acceleration was likely proportional to the product of the penetrometer diameter and initial impact velocity squared divided by the total penetrometer mass. Thus, the maximum acceleration in g's was plotted versus DV^2/M, where D is the diameter of the penetrometer in meters, V is the velocity in m/s, M is the total mass of the penetrometer in kg, and α is an empirical constant to be determined. Thus, the peak acceleration in the test data follows the empirical relation:

$$A_p = \alpha DV^2/M$$

This empirical relationship can be useful in conceptual design studies to estimate peak accelerations for soft clay impacts. Consistent results for test and analysis are obtained over a wide range of values including penetrometer size, mass, and initial impact velocity. These acceleration estimates should be conservative as the analytical results are based on a rigid penetrometer, whereas the actual vehicle may include energy absorbing structure in the design.

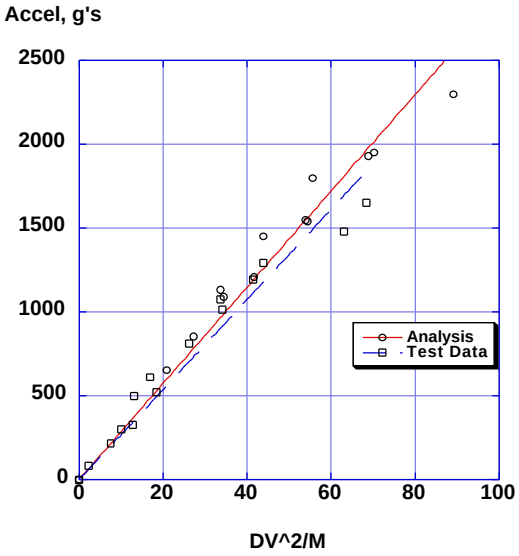

Fig. 13. Peak acceleration of penetrometer test data and analysis plotted against DV^2/M. A linear fit to each set of data is shown.

In Figure 13, both the experimental and analytical peak accelerations were plotted versus DV^2/M. Linear curve fits were made to both the test and analytical data. The slope of the test data gives $\alpha = 27$, while the slope of the analytical data is slightly higher at 29. The results show good agreement between test and analysis for these drops into clay. If the density of the soil were lowered, the

analysis would match the experimental data even better.

Soil Plastic Stress Contour

Finally, the effective plastic stress contour of the soil for the 0.66-m penetrometer at the end of the simulation (25 ms) is shown in Figure 14. True-scale deformations are shown. This view is a slice through the center of the model in order to visualize the stress state in the soil under the penetrometer. These results indicate that the domain used for the soil model appears to be adequate, and that the soil moves out of the path of the penetrometer and flows in the direction of least resistance – along the yielded material to the soil surface. Cratering of the soil on the surface near the impact site is evident.

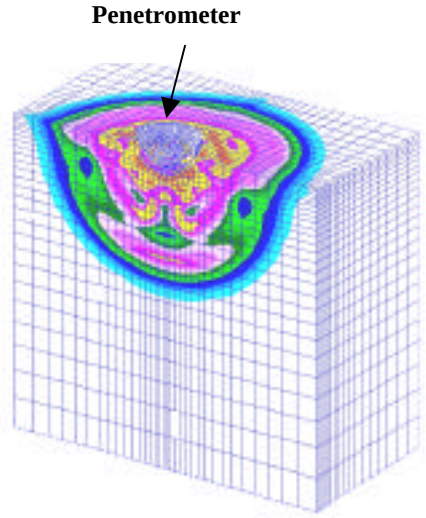

Fig. 14. Effective plastic stress at 0.025 seconds for 45 m/s impact of 0.66-m penetrometer.

Concluding Remarks

A series of penetrometer drop tests was performed into clay at the Utah Test and Training Range with different penetrometer sizes, masses, and impact speeds. These tests were simulated using the nonlinear transient dynamic finite element code, MSC.Dytran, to help characterize the expected impact response of future space exploration sample-return-mission vehicles into Earth soil without a parachute.

Pre-test predictions of the peak acceleration for the tests were made. The predicted peak accelerations using an elastic-perfectly-plastic material model for the soil compared very favorably with the test data. However, the acceleration dropped off too quickly after the peak. By adding a 20% hardening modulus to the soil material model, the pulse after the peak was simulated much more accurately.

In the analytical model, the master contact surface was defined to be the top surface of the soil, and the slave nodes were defined to be the nodes forming the rigid penetrometer. The MSC.Dytran results were found to be sensitive to the mesh discretization in the contact zone and to the contact penalty factor FACT. The best results were obtained by reducing the contact penalty factor by two orders of magnitude from the default value (from 0.1 to 0.001).

The peak accelerations for the drops of different sized penetrometers with different payloads and differing impact velocities were found to vary linearly when plotted as a function of DV^2/M (the penetrometer diameter multiplied by the impact velocity squared and divided by the penetrometer mass). This empirical relation can be useful in conceptual design studies to estimate peak accelerations. Consistent results for test and analysis were obtained over a wide range of values including penetrometer size, mass, and initial impact velocity.

Acknowledgement

The authors wish to thank Dr. Robert A. Mitcheltree and Stephen J. Hughes of NASA Langley Research Center for the penetrometer test data and support. The work performed by the last two authors was sponsored by NASA Langley Research Center under GSA Contract No. GS-35F-4503G, Task 1418. This support is gratefully acknowledged.

References

1. Mitcheltree R. A. and Kellas S., "A Passive Earth-Entry Capsule for Mars Sample Return," Symposium on Atmospheric Reentry Systems, Arcachon France, March 1999.

2. Young, C. W., “Low Velocity Earth Penetration Study – Wendover Operation,” Sandia Laboratories, Report No. SC-TM-66-2611A, April 1967.

3. McCarty, J. L and Carden, H. D.: “Response Characteristics of Impacting Penetrometers Appropriate to Lunar and Planetary Missions.” National Aeronautics and Space Administration, Washington, D.C. NASA TN D-4454, April 1968.

4. MSC.Software Corporation, "MSC.Dytran Version 4.7 User's Manual," Volumes 1 and 2, 2000.

5. Otto, O. R., Laurenson, R. M., Melliere, R. A., and Moore, R. L.: "Analyses and Limited Evaluation of Payload and Legged Landing System Structures for the Survivable Soft Landing of Instrumented Payloads." NASA CR-111919, July 1971.

6. Chen, W. F.: "Constitutive Modelling in Soil Mechanics." *Mechanics of Engineering Materials*, C. S. Desai and R. H. Gallagher (editors), John Wiley, 1984, pp. 91-120.

7. Chen, W. F. and Mizuno, E.: *Nonlinear Analysis in Soil Mechanics – Theory and Implementation*, Elsevier, Amsterdam, 1990.